Available online at www.sciencedirect.com
SCIENCE DIRECT®
International Journal of Heat and Fluid Flow 27 (2006) 135–143
International Journal of HEAT AND FLUID FLOW
www.elsevier.com/locate/ijhff

Characterization of fluid dynamic behaviour and channel wall effects in microtube

G.P. Celata [a,*], M. Cumo [b], S. McPhail [a], G. Zummo

[a] *ENEA, Institute of Thermal Fluid Dynamics, Via Anguillarese 301, 00060 Santa Maria di Galeria, Rome, Italy*
[b] *University of Rome 'La Sapienza', Corso Vittorio Emanuele II, 244 Rome, Italy*

Received 11 December 2004; received in revised form 28 March 2005; accepted 28 March 2005
Available online 16 June 2005

Abstract

Sometimes contradictory results available for fluid flow in micropipes show that much is yet to be verified in microfluid dynamics. In this study the influence of channel wall roughness and of channel wall hydrophobicity on adiabatic flow in circular microchannels is investigated, varying in diameter from 70 μm to 326 μm. The hydrodynamic behaviour of water in smooth tubes down to 30 μm inner diameter (ID) is also ascertained. Within the current experimental accuracy it is found that the classical Hagen–Poiseuille law for friction factor vs. Reynolds number is respected for all diameters measured and $Re > 300$. With degassed water, no effect of slip flow due to hydrophobic channel walls was noted even at 70 μm ID, which might suggest that the liquid slip flow phenomenon is associated with local desorption of dissolved gases on the hydrophobic surface, as reported elsewhere in the literature. For roughened glass channels, an increase in Darcy friction factor above $64/Re$ was observed only at the smallest diameter measured, 126 μm. Although the roughness levels of these channels were up to 10 times coarser than the untreated, smooth glass tubes, probably the higher factor was caused by actual deformation of channel circularity, rather than increased friction at the rougher wall, as similar behaviour was observed in a Teflon tube, also of imperfect circularity of cross-section.

For all experiments, no anticipated transition to turbulent flow was observed, which means that the transitional Reynolds number was always found between $Re \approx 2000$ and $Re \approx 3000$.

Finally, an introduction to the importance of viscous dissipation in microchannels is added, with quantitative indications of its influence on hydrodynamic properties. It is put forward as being an alternative to pressure measurements in the characterization of the behaviour of microscopic flow.

1. Introduction

In recent years, research in the field of thermal-hydraulics at microscale level has been increasing constantly due to the rapid growth of technology applications which require to transfer high heat rates in a relatively small space and volume. Such applications spread from compact heat exchangers, to cooling systems for computer CPUs, to microfluidic devices. Generally, the classical thermal and fluid dynamic theories developed for "macro systems" are not applicable to fluid in microscale structures. Furthermore, the relatively few works available in the literature in the field of microscale thermal-hydraulics reveal that there are still relevant disagreements among the results. A state-of-the-art review of fluid flow experiments in micropipes is recently given by Celata (2003).

Mala and Li (1999) investigated experimentally the flow characteristics of water in microtubes with diameters ranging from 50 to 254 μm. For tubes with smaller diameters the experimental results on friction factor show a significant departure from conventional theory,

* Corresponding author. Tel.: +39 06 3048 3905; fax: +39 06 3048 3926.
E-mail address: celata@casaccia.enea.it (G.P. Celata).

0142-727X/$ - see front matter © 2005 Elsevier Inc. All rights reserved.
doi:10.1016/j.ijheatfluidflow.2005.03.012

Nomenclature

A	cross-section, m^2
c_p	specific heat, J/kg K
d	channel diameter, m
dp/dl	pressure gradient, Pa/m
f	friction factor, –
L	channel length, m
P	perimeter, m
p	pressure, Pa
q_w	heat losses, W/m^2
r	channel radius variable, m
R	channel wall radius, m
Re	Reynolds number, $\rho uD/\mu$
u	liquid velocity, m/s
z	flow axis, m

Greek symbols

ΔT	temperature difference, K
Γ	mass flow rate, kg/s
ε	surface roughness, m
λ	thermal conductivity, W/m K
μ	dynamic viscosity, kg/m s
ρ	liquid density, kg/m^3
σ	standard variation, –

Subscripts

f	pertains to friction
in	inlet
out	outlet
tr	transition

while for tubes with greater diameters the experimental results are in good agreement with classical theory. The authors explained the unusual phenomena introducing the roughness viscosity model which takes into account the increase of momentum transfer in the boundary layer near the wall due to the presence of roughness.

Xu et al. (1999) performed experimental and theoretical investigations on water flow in microchannels with hydraulic diameter ranging from 50 μm to 300 μm and Reynolds number ranging from 50 to 1500. Experimental data revealed that flow transition did not occur in this Reynolds number range. The authors observed the flow characteristics to deviate from conventional theory when channel dimensions were below 100 μm.

In Peng and Wang (1993), Wang and Peng (1994), Peng et al. (1995) and Peng and Peterson (1996) authors performed different experimental tests of water and methanol flow and heat transfer in microchannels with hydraulic diameter ranging from 300 μm to 750 μm. The microchannels were obtained by machining of metal plates. The authors found that liquid properties and channel geometry significantly influenced the flow transition and heat transfer. The flow transition was in the Reynolds number range 700–1100.

Yu et al. (1995) reported the fluid flow characteristics of nitrogen gas and water in microtubes with diameters of 19, 52, and 102 μm and Reynolds number ranging from 250 to 20,000. In laminar flow, the friction factor was lower than that predicted by Navier–Stokes equations, while the transition laminar to turbulent flow occurred in the range $2000 < Re < 6000$.

Li et al. (2000) studied the frictional characteristic of water flowing in capillary tubes with diameters ranging from 80 μm to 205 μm. Three different materials (glass, silicon, and stainless steel) were employed in the experiments in order to verify the effect of surface roughness on hydraulic characteristics. The experimental results with smooth tubes made of glass and silicon showed that in laminar flow the friction factor was in good agreement with classical theory. Experiments with stainless steel tubes, characterised by a higher relative roughness, revealed a product fRe 15% higher than 64 in laminar flow. The transition from laminar to turbulent flow occurred for Re ranging from 1700 to 2000 and no early transition effects were observed.

Judy et al. (2000) investigated the frictional characteristics of water, hexane, and isopropanol flowing in fused silica capillaries. With the three different fluids tested, the authors studied the effect of fluid polarity on the frictional characteristics in microtubes. Capillary diameters were in the range of 20 μm to 150 μm. The authors found that for tube diameters lower than 100 μm, the friction factor deviated from classical theory significantly. The deviation was independent of Re and depended on the tube diameter. In particular, friction factors were lower than expected and the deviations were lower as the tube diameter decreased, reaching 30% deviation from classical theory for 20 μm tubes.

Judy et al. (2002) performed very accurate experiments on frictional characteristics of fluid flow in microtubes. The capillary diameters varied from 15 up to 150 μm and three different fluids, water, methanol, and isopropanol, were tested. The authors concluded that the experimental results were in good agreement with classical theory. The value of fRe could be considered equal to 64, considering the experimental error, and it was independent of Reynolds number for $Re < 2000$. The latter finding showed that the transition from laminar to turbulent flow regime did not occur for Reynolds lower than 2000.

Wu and Cheng (2003) focused on the influence of aspect ratio in trapezoidal, hydrophobic silicon microchannels with hydraulic diameters between 26 μm and

291 μm. They found a great dependence of hydraulic friction factor on the cross-sectional aspect ratio, but within this, a close adherence to the Navier–Stokes equations (that yield the classical value of 64/*Re* for the friction factor in circular ducts) for all diameters in the laminar regime. No mention was made of liquid slip flow effects.

Celata et al. (2002) reported the results of R114 flowing in capillary tubes with an internal diameter of 130 μm. They found the friction factor was in good agreement with the Hagen–Poiseuille theory for Reynolds number below 600–800. For higher values of Reynolds number, experimental data depart from the Hagen–Poiseuille law to the side of higher friction factor values. The transition from laminar to turbulent regime occurs for Reynolds number in the range 1900–2500. Similar results have been obtained by Bucci et al. (2003) using water in micropipes from 290 to 500 μm.

The objective of the present study is to set out our experimental verifications of the influence of channel wall conditions on adiabatic flow in circular microchannels varying in diameter from around 100 μm to 400 μm. The two surface conditions studied are roughened and siliconated glass walls—compared with otherwise smooth glass ducts. Furthermore, the results of a hydrodynamic characterization of water flow in smooth tubes down to 30 μm inner diameter (ID) is presented. An introduction to the aspect of viscous heating and its importance in microchannel flow is added for this purpose.

2. Experimental set-up

Experiments are carried out using demineralised water, which is degassed by passing through a very small, but continuous quantity of helium. Being insoluble in water, an atmosphere of only helium is created above the liquid level, so that all dissolved gases are driven out by their respective partial pressures in the water. A schematic of the test loop is shown in Fig. 1. After being filtered of solid impurities through a 10 μm filter, the water passes through a gear pump—for flow rates over 10 ml/min and pressures below 6 bars—or a piston pump with damper—for conquering the large pressure drops through the smallest diameters (up to 120 bars for a 30 μm tube) at flow rates below 25 ml/min. The water is then, if desired, brought to a certain controlled temperature level with a Peltier cell type pre-heater. This can be convenient to reduce water viscosity and thus head loss.

A 250 μm K-type thermocouple verifies the actual fluid temperature on entrance into the test section, and pressure transducers on either side of the microtube investigated allow the pressure drop over the channel to be established. The mass flow rate is measured with a high precision scale.

The adopted means of measuring the frictional pressure drop per unit of length in the microchannel, therefore without inlet and outlet effects, is schematised in Fig. 2.

For each type of capillary studied, two lengths are cut from the same tube (so that surface conditions on the inside can be assumed comparable) and mounted in identical fittings. Thus, at equal mass flow rates, the concentrated pressure losses ΔP_{in} and ΔP_{out} must be the same for the two lengths of tube. Therefore, subtracting the total pressure drop along the shorter tube from that measured by the transducers for the longer tube, the difference yields the frictional pressure loss over the extra length of capillary ($dp/dl * \Delta L$).

Then, in the Darcy equation

$$f = 2\frac{\Delta p}{\Delta L}\frac{d}{\rho u^2} \tag{1}$$

the friction factor f for the type of capillary under consideration, can be calculated inserting this difference for Δp, and the difference in length for ΔL. Obviously, the respective lengths of the two tubes are always made to be long enough for fully developed flow to settle. The dimensionless hydrodynamic entrance length is dependent on the Reynolds number for laminar flow: $0.055 * Re$ (Shah and London, 1978). The maximum value is therefore at $Re \approx 2200$: 120 diameters. The length

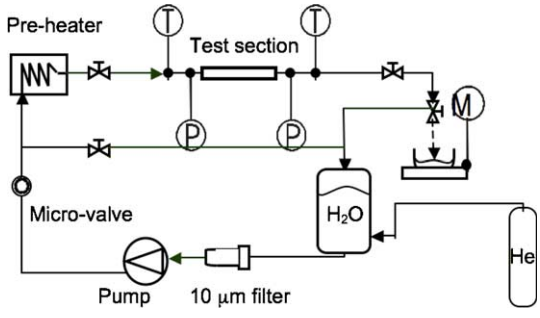

Fig. 1. Schematic of test-loop.

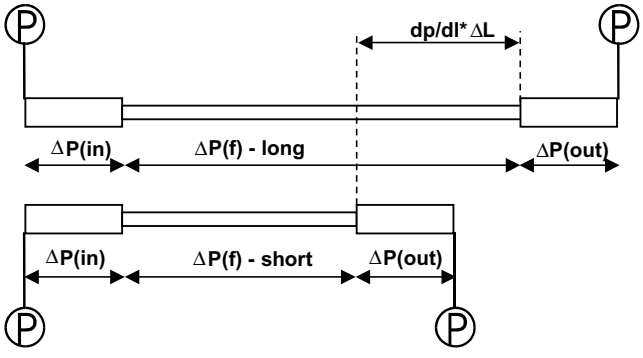

Fig. 2. Pressure loss distribution along long and short test sections.

of the short tube is at least 350–400 diameters, so that in the subtraction of the gross pressure drops the hydrodynamic entrance length effects (which, it is remembered, are considered identical for the two lengths of tube at equal mass flow rates) are cancelled quite comfortably. The difference in length ΔL, typically 100–300 diameters, will then always be representative of frictional head loss only.

The bulk fluid velocity u in Eq. (1) is calculated as

$$u = \frac{\Gamma}{\rho A},$$

where A is the cross-sectional area of the microtube, ρ is the fluid density and Γ the mass flow rate.

2.1. Overview of capillaries tested

First, to verify the adherence of fluid flow to classical theory also in microscale in regular circular channels, fused silica tubes were tested down to 30 μm ID. Thus, also a reference was established for the hydrodynamic tests on tubes with surface treatment.

The effect of surface roughness was studied. To this end smooth glass tubes ($\varepsilon \approx 0.05$ μm) were roughened on the inside using fine-grain abrasive powder and fluid silicon oil, in a weight ratio of between 1:1 and 1.5:1. This mixture was introduced in the capillary tube with a fine steel thread, and in a to-and-fro motion of about 30 cycles, the entire length of the capillary tube (about 15 cm) was 'filed', roughening the inner surface. Glass tubes of 300 μm and 130 μm nominal ID were treated resulting in an order of absolute roughness of $0.2\ \mu\text{m} < \varepsilon < 0.7\ \mu\text{m}$ (the nature of the process prohibits the realisation of perfectly uniform roughness along the tube). In *relative* terms this still approximates smooth tubes (that is, $\varepsilon/D < 1\%$), but compared to the absolute roughness of untreated glass tubes ($\varepsilon \approx 0.05$ μm), it is nevertheless a distinct increase. The roughness was measured with an electronic Profilometer (ZYGO NewView 5000) based on optic interferometry and with an accuracy on height of 10 nm.

In Fig. 3(a)–(d) the Scanning Electron Microscope (SEM) images of the cross-sections of four types of capillaries tested are represented.

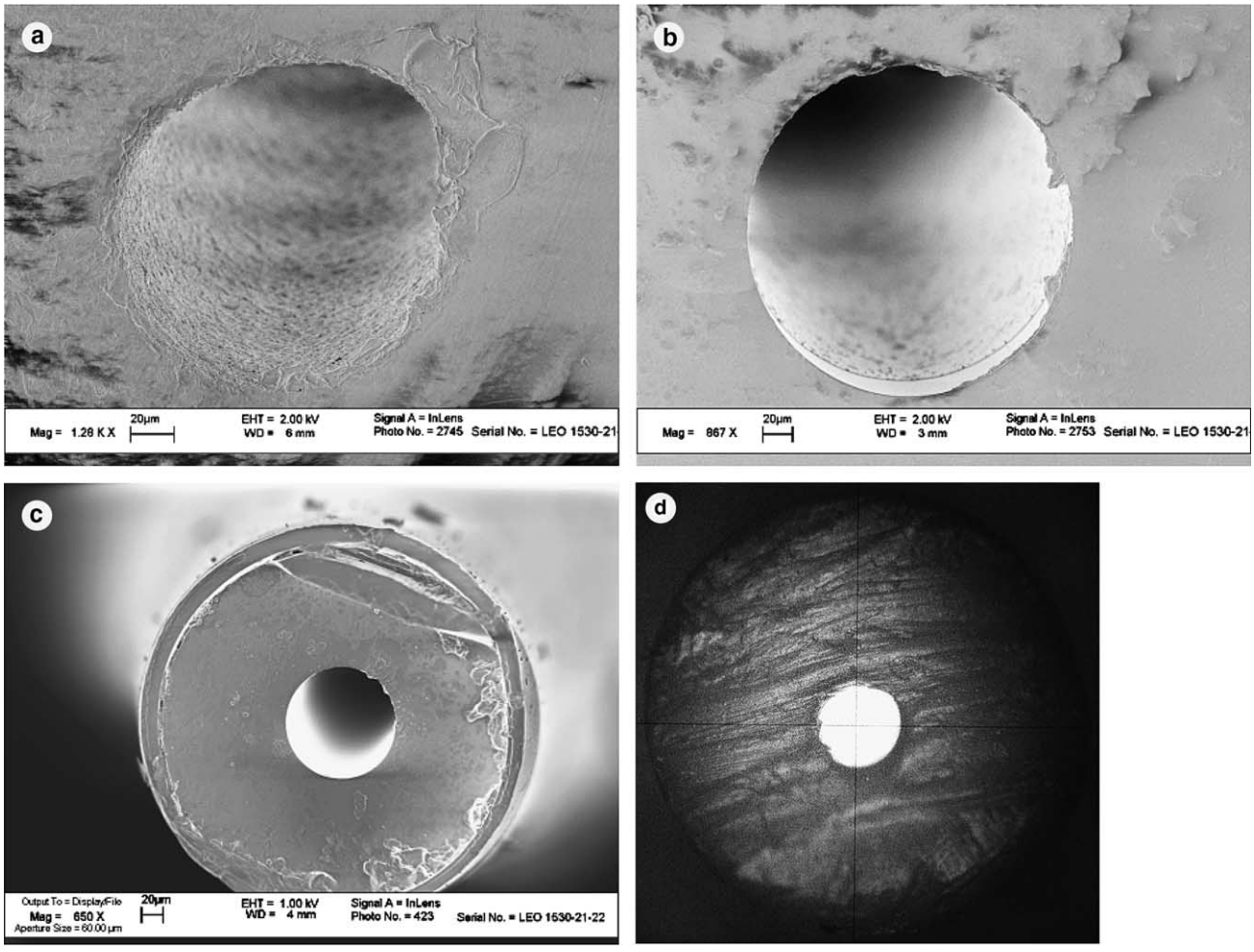

Fig. 3. (a) Cross-section of a roughened glass capillary. (b) Cross-section of a siliconated glass tube. (c) Cross-section of a fused silica capillary. (d) Cross-section of a Teflon tube.

Table 1
Parameters of investigated channels

Channel	Diameter (μm)	Error (μm)	Material	Surface
#1	31	±0.82	F.S.	–
#2	50	±2.6	F.S.	–
#3	101	±2.5	F.S.	–
#4	259	±8.2	Glass	–
#5	70	±0.9	Glass	Siliconated
#6	116	±1.7	Glass	Siliconated
#7	326	±1.8	Glass	Siliconated
#8	300	±19	Teflon	–
#9	126	±6.5	Glass	Roughened
#10	300	±6.4	Glass	Roughened

To investigate the effect of hydrophobic channel walls on water flow, a thin layer of silicon was applied on the inside of glass tubes varying in diameter from 330 μm down to 72 μm (following the technique set out by Grob, 1986). The resulting final diameters are those in Table 1. Where the wall is non-wettable (hydrophobic), slip condition would be expected to exist, i.e. non-zero fluid velocity at the wall. This means less viscous deformation in the fluid and therefore less pressure loss within the channel. Tests for liquid slip flow effects were also done on a Teflon tube, the cross-section of which is represented in Fig. 3(d).

The types of channels investigated in this study are listed in Table 1 (F.S. stands for fused silica). The tube diameters were measured through image analysis of the SEM pictures and are averaged values of several cross-sections of the same tube. The variance depends on the kind of capillary and is in fact due to slight non-uniformity of the diameter across the length of the test sample, rather than to an inaccuracy in the SEM visualization. The Teflon tube (#8) therein had the highest deviation from the mean, in that both the shape of the cross-section varied notably along the axis, as also the (equivalent) diameter. The inaccuracy is around 20 μm for this tube.

3. Uncertainty analysis

In order to analyse the influence of the experimental parameters on friction factor, it is convenient to perform an uncertainty analysis of the variable of interest, f. The friction factor is calculated with the Darcy equation (1). Transcribing so that all variables are measurable entities we obtain the expression:

$$f = \frac{\pi^2}{8}\frac{\rho\Delta p d^5}{L\Gamma^2}, \tag{2}$$

where Δp is the pressure loss across the pipe, d is the pipe diameter, L is the pipe length, ρ is the fluid density, and Γ is the mass flow rate.

According to the Taylor expansion procedure described also in Celata (2003) the uncertainty analysis on f, which gives the relative estimation of error e_f due to the uncertainties in the independent variables, is the following:

$$\left(\frac{e_f}{f}\right)^2 = \left(\frac{1}{\rho}e_\rho\right)^2 + \left(\frac{1}{\Delta p}e_{\Delta p}\right)^2 + \left(\frac{5}{d}e_d\right)^2 + \left(\frac{1}{L}e_L\right)^2 + \left(\frac{2}{\Gamma}e_\Gamma\right)^2, \tag{3}$$

where $e_{\Delta p}$, e_d, e_L, e_ρ, and e_Γ are the uncertainties in the respective independent variables, so that for each condition of experiment the corresponding relative error can be computed.

In Eq. (3), the term $((5/d)e_d)^2$ plays an important role in the uncertainty of the friction factor due to the presence of the factor 5 and the small value of channel diameter in the denominator. The influence of this term can be dramatic for diameters lower than 100 μm and accuracy in diameter measurement of ±1 μm, as was already shown in the cited article.

When introducing slip at the channel wall, the laminar velocity profile is shifted along the direction of flow (Tretheway et al., 2002):

$$u = -\frac{R^2}{4\mu}\left(\frac{\partial p}{\partial x}\right)\left[1 - \left(\frac{r}{R}\right)^2 + \frac{2\beta}{R}\right]. \tag{4}$$

The parameter which describes this is the slip length, β, which is an indication of the amount of slip with respect to the classic assumption of zero-velocity at the wall. The solution to Eq. (1) then, is not $64/Re$ as for the classical case (Fox and McDonald, 1994), but becomes:

$$f = \frac{64\mu}{\rho u(d - 2\beta)}. \tag{5}$$

In this way one can establish the magnitude of the effect that slip flow would have on flow resistance. In an f-vs.-Re plot (like e.g. Figs. 4–9) increasing or decreasing the value of the diameter (an effect that uncertainties

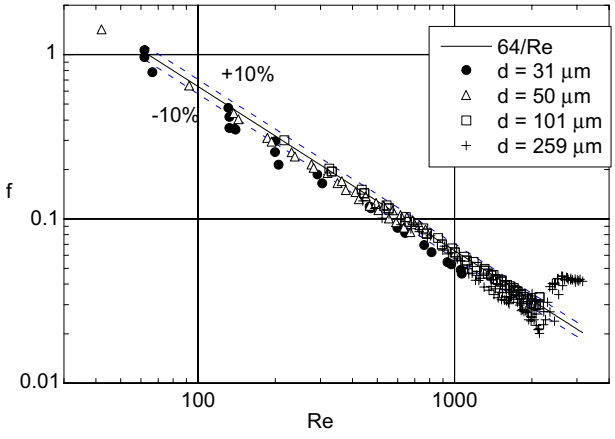

Fig. 4. Friction factor, f, versus Reynolds number, Re at various diameters: untreated smooth tubes.

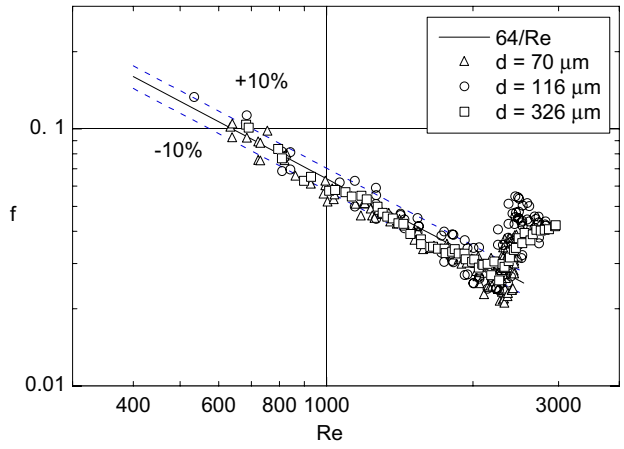

Fig. 5. Friction factor, f, versus Reynolds number, Re at various diameters: siliconated smooth tubes.

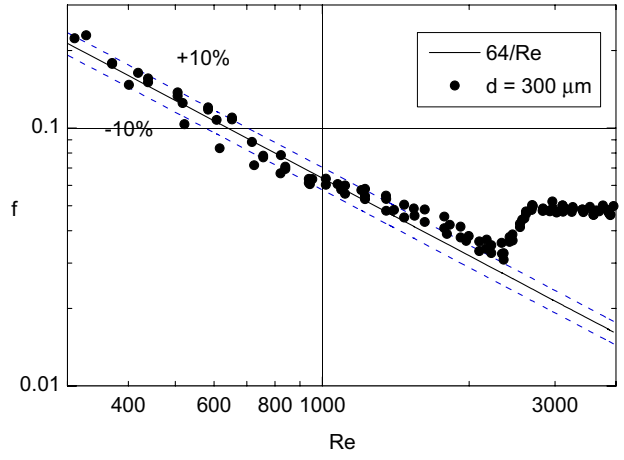

Fig. 6. Friction factor, f, versus Reynolds number, Re: Teflon tube.

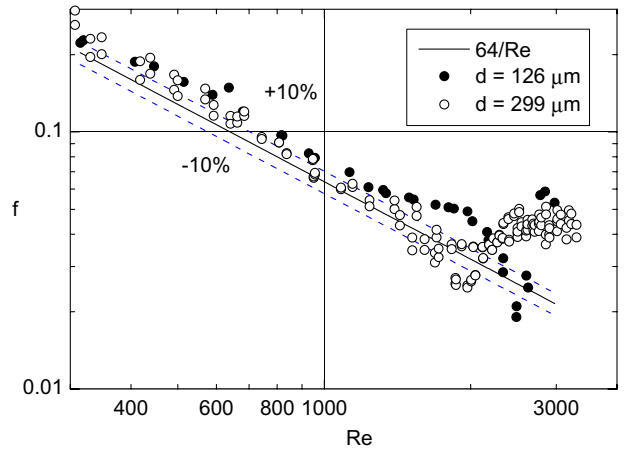

Fig. 7. Friction factor, f, versus Reynolds number, Re at various diameters: roughened glass tubes.

may have) translates data points respectively up or down compared to the reference line $f = 64/Re$. The effect of slip flow is synthesised in Eq. (5) as a correction on the pipe diameter, so that the slip length β must be larger than the error on diameter measurements for it to be noticed reliably in experiments. Thus, from their values in Table 1, one can directly infer the minimum slip length discernible. In Tretheway et al. (2002), for 55 μm hydraulic diameter hydrophobic channels, Particle Image Velocimetry detected a slip length β of almost 1 μm, so that effects might just be visible at the diameter accuracies reported in Table 1.

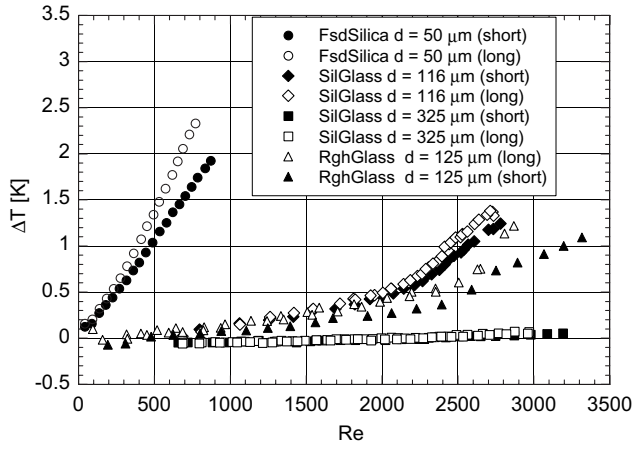

Fig. 8. Temperature rise versus Reynolds number in selected test sections.

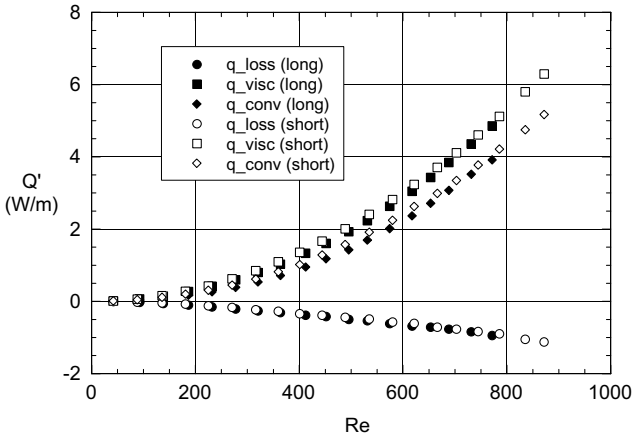

Fig. 9. Heat flux distribution per unit length in channel #2 (Eq. (9)).

4. Results and discussion

The friction factors are presented in Fig. 4 as a function of Reynolds number for the untreated, smooth tubes (#1 to #4).

It can be noted that from $Re > 300$, for all diameters, the friction factor data follow the theoretical Hagen–Poiseuille curve near perfectly. For the smallest diameter

(31 μm) the experimental error margin is larger (±19%), so the friction factor at low Reynolds numbers can also still be considered within applicability of the 64/*Re* law. The upper limit of fluid velocity for channel #1 was determined by the maximum pump head pressure, preventing the reaching of transition. For the larger smooth tubes, no anticipated transition from laminar to turbulent flow was observed.

Our experiments on hydrophobic channel walls, as in the siliconated glass tubes #5 to #7, appear to deny any effect of slip condition on global friction factor for all diameters and Reynolds numbers tested, as is shown in Fig. 5, where the friction factor is plotted versus Reynolds number. Apart from a slightly larger dispersion around the 64/*Re* line before transition—which in its uniform distribution illustrates clearly the phenomenon of experimental uncertainty—behaviour is classical. As diameters decrease the onset of turbulent flow is more sudden, but consistently within the range of $2000 < Re < 3000$.

Research by Tretheway et al. (2002) on the exact mechanism of slip flow suggested that the apparent fluid slip at a hydrophobic wall may result from the presence of nanobubbles at the surface. Their experiments demonstrated through Particle Image Velocimetry that there is a significant slip velocity at the wall of water flowing through a 55 μm hydraulic diameter channel, over a monomolecular hydrophobic surface. (Our tubes are coated with an extra layer of methylsilicone above the monomolecular layer to ensure durability of the non-wettable layer at high pressures.) This is replicable using a model that stipulates an air gap between fluid and channel wall, which induced them to propose the desorption mechanism. However, their experiments were conducted with deionised water untreated for the removal of dissolved or entrained gases. The results obtained by us for degassed water (which show no apparent slip effect) might therefore be a verification of their suggested theory. Although the dimensions of their duct were smaller than what we were able to have treated reliably, the absence of any visible effect within the experimental error band indicates that the slip length (if extant) is below the dimensions of the accuracies on diameter measurements (assuming these are dominant with respect to the other variables in Eq. (2)).

The results for the Teflon tube are plotted in Fig. 6, where the Reynolds number and friction factor were calculated with the mean measured equivalent diameter of 304 μm. Rather than any slip effect of the non-wettable surface, the graph proves there must be an influence of cross-sectional contractions and dilations on the friction factor along the tube length for the range of Reynolds numbers tested, which explains the increased friction experienced between $1000 < Re < 2000$. One cannot speak of anticipated transition though, as the jump towards turbulent regime is very well defined at $Re \approx 2300$.

The results for roughened tubes (#9 and #10) are presented in Fig. 7, where, again, friction factor is plotted versus Reynolds number. At 300 μm ID, the friction factor follows, within the range of experimental accuracy, the Hagen–Poiseuille law. The smallest tube that it was physically possible to realise with the roughening process described above, does seem to show an effect of increased resistance on fluid flow, even at a low relative roughness value ($\varepsilon/d \approx 0.1\%$). On consideration, and on observing scanning electron microscope images like Fig. 3(a), it seems more probable that actual deformation of the circularity of the channel cross-section is the cause of this. Elliptical channels have a higher friction factor than circular ones (Shah and London, 1978). In addition to this, the smaller capillary seems to manifest the same rise in frictional loss between $1000 < Re < 2000$ as was observed in the Teflon tube of non-constant shape and diameter. This serves to stress further the weight of channel diameter, but also of geometry precision in the accurate prediction of microtube phenomenology. Precisely the factors that are most difficult to manage at this scale.

Transition to turbulent flow seems to occur later for channel #9 (and more abruptly) than for channel #10. According to the empirical method for calculating the boundaries of laminar-to-turbulent flow by Preger and Samoilenko (1966), as reported by Idelchick (1986), the transition region is delimited by the following two *Re* values:

$$Re_1 = 1160\left(\frac{1}{\varepsilon/d}\right)^{0.11}, \tag{6}$$

$$Re_2 = 2090\left(\frac{1}{\varepsilon/d}\right)^{0.0635}. \tag{7}$$

For the 300 μm roughened capillary ($\varepsilon \approx 0.7$ μm) the transition zone is calculated to be between $Re_1 = 2260$ and $Re_2 = 3070$. In the case of the 126 μm channel ($\varepsilon \approx 0.16$ μm) Eqs. (3) and (4) predict transition between $Re_1 = 2400$ and $Re_2 = 3200$, at a relative roughness which is lower than for the larger tube. These values correspond acceptably to those discernable in Fig. 7, although no effect of abruptness is indicated by the equations.

5. Viscous heating

An evaluation of viscous heating in the fluid, due to the high pressure drop in the micropipe, has been attempted.

In steady state, the energy balance for channel flow is generalized as:

$$\rho c_p u \frac{\partial T}{\partial z} = \lambda \nabla^2 T + \mu \left(\frac{\partial u}{\partial r} \right)^2, \tag{8}$$

where the left-hand term is the convective transport through the channel (along the axis, z), and on the right-hand side are summed the conductive heat loss and the viscous heat generation. With the assumptions of: circular channel cross-section, fully developed laminar (Poiseuille) velocity profile and constant fluid properties along the tube length, upon integration over the cross-sectional area of the microtube, A, the balance reduces to:

$$\rho c_p A \frac{\Delta T}{L} u = q_w P + 8\pi\mu u^2, \tag{9}$$

where q_w is the heat flux at the walls of the microtube (positive if the fluid is heated) and P is the perimeter of the cross-section. From this equation it is possible to determine the specific heat loss, q_w [W/m^2], to the surroundings, as the viscous heat production is explicit in the right-most term. The temperature difference, ΔT, between outlet and inlet of a few representative channels as a function of Reynolds number is shown in Fig. 8.

As would be expected, there is a larger fluid temperature rise in the smaller channels, increasing with fluid velocity. One naturally assumes this to be mainly the consequence of viscotic heat production. If we apply Eq. (6) to the data of the 50 μm ID fused silica tube, the following distribution of the heat fluxes is observed (Fig. 9).

We can see in fact that the heat production and dissipation are constant per unit of length—which is why the respective curves for the long and short tube are equivalent—and depend quadratically on fluid velocity (or: Reynolds number where channel and fluid properties are constant). The heat loss to the surroundings acts as a stabilizing factor in the thermal conditions of the channel, so that isothermal flow is more closely approximated. Nevertheless, it is evident that viscous heating becomes rapidly of importance at diameters below 100 μm and would need to be evaluated in the case of sensitive heat transfer applications. For fluid-dynamic considerations, viscous heating will influence the value of the Reynolds number through changes in viscosity and density caused by the temperature rise. From the calculations here above, the maximum variation of the Reynolds number (50 μm pipe), with respect to the average value is ±2.5%. The Reynolds number used for calculation is the average value obtained from measured outlet and inlet temperature, so that it can be said to account for the effect of viscous dissipation. More importantly, this energy transformation is directly linked to viscous deformation of the fluid layers and thus must equally provide information on the friction factor as pressure measurements would. This way, a possibility of determining friction factors in microscopic geometries is created which by-passes the implementation of cumbersome pressure transducers in the system. A detailed analysis of this aspect is under publication in a dedicated article.

6. Conclusions

Hydrodynamic tests were carried out on smooth, glass/fused silica capillary tubes from 259 μm down to 31 μm ID, to establish any deviation from the classical Hagen–Poiseuille law ($f = 64/Re$ for circular channels) in the microregime. Within the range of our experimental accuracy a definite adherence is verified, in any case from $Re > 300$, for all diameters.

Various studies have taken place recently regarding the phenomenon of slip flow and the influence of hydrophobic surfaces on frictional pressure drop. These have been shown to be significant at very small diameters ($d < 100$ μm), but the actual mechanism of slip flow is not completely clear. In dealing with the slip condition, the so-called *slip length* emerges, which enters into the solution for the friction factor as a correction on the channel diameter. The results by us obtained with *degassed* water seem to indicate no reduction in fluid friction for tubes down to 70 μm ID, or at least a slip length which is lower than the values of inaccuracy on diameter measurements. In conjunction with conjectures by other researchers, this might explain the actual physics of fluid slip as being caused by the presence of desorbed nanobubbles on the hydrophobic surface.

As for the effect of surface roughness, it has become apparent that of far greater importance is the ''deformity'' of the channel geometry. At microscopic scale, it is unlikely to have a *uniform* asperity in the duct that does not influence the actual *shape* of the cross-section more heavily than attribute a symmetrical degree of roughness to the wall. Thus, it was found that the roughened channels did not show any diversion from the classic prediction that denies effects of wall roughness on friction factor in laminar flow. What differences were encountered, are more probably the result of deviations from the circular geometry of the test sections—as the same effect was observed quite strongly in a smooth, hydrophobic channel that was demonstrably non-perfectly circular.

Acknowledgements

The help of Romualdo D'Angelo, MSc, for the work on smooth, untreated tubes, as well as for the fine-tuning of the test rig for all subsequent experiments is highly appreciated. Gratitude is also due to Dr. Luigi Nardi for the treatment of the capillaries and to Dr. Emanuele Serra for the SEM measurements.

Part of this paper is made possible by the EU, Framework Project HMTMIC, RTN Contract HPRN-CT-2002-00204.

References

Bucci, A., Celata, G.P., Cumo, M., Serra, E., Zummo, G., 2003. Fluid flow and single-phase flow heat transfer of water in capillary tubes. In: Proceedings of the International Conference on Minichannels and Microchannels, Paper ICMM-1037, Rochester, April 24–25.

Celata, G.P., 2003. Single-phase heat transfer and fluid flow in micropipes. In: Proceedings of the 1st International Conference on Microchannels and Minichannels, Rochester, New York, April 24–25.

Celata, G.P., Cumo, M., Guglielmi, M., Zummo, G., 2002. Experimental investigation of hydraulic and single phase heat transfer in 0.130 mm capillary tube. Microscale Thermophys. Eng. 6, 85–97.

Fox, R.W., McDonald, A.T., 1994. Introduction to Fluid Mechanics. John Wiley & Sons, New York, p. 330 & f.

Grob, K., 1986. Making and Manipulating Capillary Columns for Gas Chromatography. Huethig, Heidelberg.

Idelchick, I.E., 1986. Handbook of Hydraulic Resistance, second ed. Hemisphere Publishing Corporation.

Judy, J., Maynes, D., Webb, B.W., 2000. Liquid flow pressure drop in microtubes. In: Proceedings of the International Conference on Heat Transfer and Transport Phenomena in Microscale, Banff, Canada, October 15–20.

Judy, J., Maynes, D., Webb, B.W., 2002. Characterization of frictional pressure drop for liquid flows through microchannels. Int. J. Heat Mass Transfer 45, 3477–3489.

Li, Z.X., Du, D.X., Guo, Z.Y., 2000. Experimental study on flow characteristics of liquid in circular microtubes. In: Proceedings of the International Conference on Heat Transfer and Transport Phenomena in Microscale, Banff, Canada, October 15–20.

Mala, G.M., Li, D., 1999. Flow characteristics in microtubes. Int. J. Heat Fluid Flow 20, 142–148.

Peng, X.F., Peterson, G.P., 1996. Convective heat transfer and flow friction for water flow in microchannels structures. Int. J. Heat Mass Transfer 39 (12), 2599–2608.

Peng, X.F., Wang, B.X., 1993. Forced convection and fluid flow boiling heat transfer for liquid flowing through microchannels. Int. J. Heat Mass Transfer 36 (14), 3421–3427.

Peng, X.F., Wang, B.X., Peterson, G.P., Ma, H.B., 1995. Experimental investigation of heat transfer in flat plates with rectangular microchannels. Int. J. Heat Mass Transfer 38 (1), 127–137.

Preger, E.A., Samoilenko, L.A., 1966. Investigation of hydraulic resistance of pipelines in the transient mode of flow of liquids and gases. Issled, Vodosnabzhen, Kanalizatsii (Trudy LISI), Leningrad 50, 27–39.

Shah, R.K., London, A.L., 1978. Laminar flow forced convection in ducts. Advances in Heat Transfer. Academic Press, New York, p. 91, 248.

Tretheway, D.C., Liu, X., Meinhart, C.D., 2002. Analysis of slip flow in microchannels. In: Proceedings of 11th International Symposium on Applications of Laser Techniques to Fluid Mechanics, Lisbon, July 8–11.

Wang, B.X., Peng, X.F., 1994. Experimental investigation on liquid forced convection heat transfer through microchannels. Int. J. Heat Mass Transfer 37 (1), 73–82.

Wu, H.Y., Cheng, P., 2003. Friction factors in smooth trapezoidal silicon microchannels with different aspect ratios. Int. J. Heat Mass Transfer 46, 2519–2525.

Xu, B., Ooi, K.T., Wong, N.T., Liu, C.Y., Choi, W.K., 1999. Liquid flow in microchannels. In: Proceedings of the 5th ASME/JSME Joint Thermal Engineering Conference, San Diego, California, March 15–19.

Yu, D., Warrington, R., Barron, R., Ameel, T., 1995. An experimental and theoretical investigation of fluid flow and heat transfer in microtubesASME/JSME Thermal Engineering Conference, vol. 1. ASME.